Primljen / Received: 18.8.2022.
Ispravljen / Corrected: 5.12.2022.
Prihvaćen / Accepted: 11.12.2022.
Dostupno online / Available online: 10.1.2023.

Upgrading of isolated bridges with uniform gapped HS devices: Seismic tests

Authors:

Assoc.Prof. **Jelena Ristić**, PhD. CE
International Balkan University (IBU)
Faculty of Engineering
Department of Civil Engineering
jelena.ristic@ibu.edu.mk
Corresponding author

Prof. **Danilo Ristić**, PhD. CE
SS Cyril and Methodius University in Skopje, Republic North Macedonia
Institute of Earthquake Engineering and Engineering Seismology (IZIIS)
danilo.ristic@gmail.com

Prof. **Viktor Hristovski**, PhD. CE
SS Cyril and Methodius University in Skopje, Republic North Macedonia
Institute of Earthquake Engineering and Engineering Seismology (IZIIS)
viktor@iziis.ukim.edu.mk

Research Paper

Jelena Ristić, Danilo Ristić, Viktor Hristovski

Upgrading of isolated bridges with uniform gapped HS devices: Seismic tests

The conducted extensive experimental seismic analysis showed seismic performances of a constructed large-scale bridge model representing system of upgraded isolated bridge with uniform gapped horizontal S-shaped devices (GHS System). The GHS system constituted double spherical rolling isolating bearings (DSRIB) and created original uniform horizontal S-shaped multi-gap (HS-MG) energy dissipation devices. With conducted laboratory cyclic tests, stable all-directional hysteretic responses were confirmed for both the DSRIB and HS-MG devices. In the dynamic seismic shaking table testing, the GHS bridge system showed favourable seismic response performances contributing to efficient bridge system protection. The established new GHS system exhibited large potential for qualitative improvement of seismic safety of isolated bridges exposed to very strong earthquakes.

Key words:
bridge, seismic isolation, energy dissipation, bridge safety, seismic shaking table

Prethodno priopćenje

Jelena Ristić, Danilo Ristić, Viktor Hristovski

Poboljšanje mostova s potresnom izolacijom primjenom horizontalnih uređaja S-oblika (HS)

Na modelu izvedenom u velikom mjerilu provedena su opsežna eksperimentalna ispitivanja na potresnu pobudu koja su pokazala odziv mosta s izolacijom poboljšanog primjenom horizontalnih uređaja S-oblika (HS) koji omogućavaju ograničene pomake (GHS sustav). GHS sustav je sastavljen od dvostrukih sfernih kotrljajućih izolacijskih ležajeva (DSRIB) i razvijenih originalnih uređaja za trošenje energije s komponentama S-oblika (HS-MG). Vrlo stabilni odzivi u svim smjerovima su potvrđeni laboratorijskim cikličnim testovima za oba uređaja, DSRIB i HS-MG. U eksperimentalnom ispitivanju na potresnom stolu, GHS izolacijski sustav mosta je pokazao povoljno ponašanje pri potresnom djelovanju pridonoseći učinkovitoj zaštiti mosta. Novi GHS sustav pokazao je veliki potencijal za kvalitativno poboljšanje sigurnosti mostova s potresnom izolacijom izloženih vrlo jakim potresima.

Ključne riječi:
most, potresna izolacija, trošenje energije, sigurnost mosta, potresni stol

1. Introduction

Although important studies related to seismic isolation of bridges have been realized in many known research centres in Japan, USA, Italy, etc., the ideas and studies from many other countries have become significant [1]. However, the conducted research mostly focused on the development of specific individual devices such as: rubber isolation devices, sliding isolation devices, rolling isolation devices, and some displacement-limiting devices, among others. Reviews of the achievements in this research field are provided in various publications [1, 2]. Performances of common rubber and lead-rubber isolation devices are presented in [3, 4]. The specific behaviour of sliding isolation devices is described in various published papers [5-7], including simple pendulum isolation devices [8, 9] and experimental tests were conducted in [10, 11]. The basic concepts of some specific devices for energy dissipation, as well as some displacement-limiting devices, have also been introduced [12-14]. Specific U-shaped hysteretic steel dampers were developed and mainly used for buildings [15-17]. Lately, new developments include studies related to phenomena and/or concepts such as pounding effects [18], axial behaviour of elastomeric isolation devices [19], or semi-active dampers [20, 21]. Design regulations for isolation of bridges have also been introduced [22, 23], and implemented worldwide in seismically prone regions [24]. Lastly, new complex systems have been studied through shaking table tests of scaled structure models [25]. Heavy seismic damage to bridges has constantly been observed during strong earthquakes. Sub-structure damage is mostly manifested by large deformations, settlements, permanent displacements, large cracks or overturning of a structure [26]. Meanwhile, superstructures are mostly significantly displaced or completely collapsed [27]. Even modern bridges suffer severe damages under strong earthquakes [28, 29]. Although there is some recorded evidence of favourable behaviour of seismically isolated bridges, it is evident that to date, not many bridges have experienced strong near-fault earthquakes [28, 30]. Recently, a great interest has manifested on instrumentation and real-time monitoring of bridges exposed to strong, near-fault ground motions. Some recent reports addressed potential problems related to isolated bridges and less-favourable behaviour. Typical abrupt damages to isolated bridges were observed on the large Bolu viaduct after the strong Duzce (Turkey) earthquake in 1999. The ruptured fault crossing the viaduct produced a significantly stronger earthquake than that designed [31, 32]. However, the viaduct resisted total collapse. For example, during the 1995 Kobe earthquake, the Higashi-Kobe bridge suffered damages related to large displacements [33], while some isolated bridges were damaged during the Great East Japan earthquake in 2011. Some smaller damages were reported to have occurred on the Thjorsa River Bridge and the Oseyarar Bridge in Iceland, following a near-fault ground motion [34]. The research results presented in this paper were obtained from an original development study resulting in creation of innovative HS-MG devices that can qualitatively contribute to avoiding safety problems under severe impacts of very strong earthquakes on isolated bridge structures.

2. The new GHS bridge system

Extensive experimental and analytical analyses were performed in the Institute of Earthquake Engineering and Engineering Seismology (IZIIS), Ss. Cyril and Methodius University (Skopje), as part of the NATO Science for Peace and Security Project "Seismic Upgrading of Bridges in South-East Europe by Innovative Technologies" (SFP: 983828), led by the second author. The developed GHS system represents a specific part of the integral research. The new gapped horizontal S-shaped system (GHS-system) has been developed based on the created compact passive HS-MG device for energy dissipation with multiple gaps to provide improved bridge response under very strong earthquakes. It was formulated by implementing the adopted concept of global optimization of the seismic energy balance. The designed HS-MG energy dissipation devices used as supplementary damping represent a qualitative system improvement respective to bridge isolation only. The GHS system is based on incorporation of three complementary systems:

- The common seismic isolation system (SI system) providing low stiffness in horizontal direction
- The new HS-MG energy dissipation system to provide sufficient damping through dissipation of seismic energy
- Displacement limiting (DL) devices to reduce or eliminate excessive displacements under strong impact effects.

The conducted research included two main parts. During the initial study, original quasi-static tests of prototype models of components and devices were performed. In the second part, seismic testing of the original GHS bridge model was performed under simulated effect of strong earthquakes. The physical bridge model was designed and constructed to be compatible for successful quasi-static and seismic shaking table testing.

3. Creation and testing of HS-MG device for energy dissipation

3.1. Prototype of HS-MG device

Considering the specific objective of the present experimental study that included creation and original testing of the innovative upgrading concept, particular attention was paid to developing a new integrated, compact and ductile upgrading unit. It structurally represents a horizontal S-shaped multi-gap (HS-MG) and all-directional energy dissipation device with large seismic energy dissipation capacity. The structure of the multi-directional HS-MG device is depicted in Figure 1, constituting three basic segments: S1) a metal base ring with a fixed side vertical support

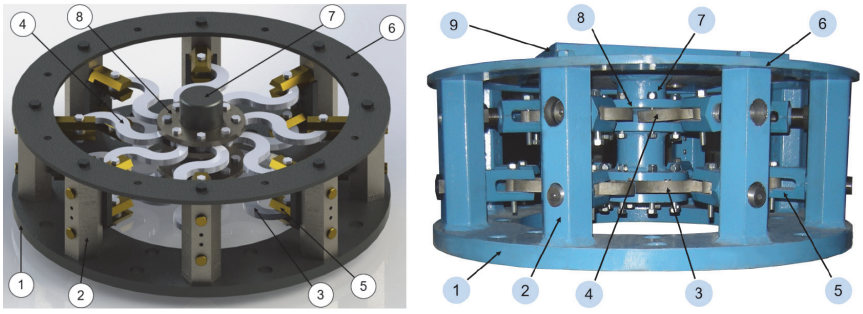

Figure 1. Prototype of designed & constructed HS-MG device: 1. Bottom fixing ring; 2. Side vertical supports; 3. HS-Components at level-L1; 4. HS-Components at level-L2; 5. Gapped support; 6. Upper ring plate; 7. Central hinge support; 8. Central activating device; 9. Upper fixing plate

system providing gap-based supports to the energy dissipation (ED) components; S2) an adequately shaped central hinge-support with a system for activation of the ED components, and S3) horizontal HS-MG energy dissipation components uniformly distributed through the two levels. The device activation and response provide beneficial effects in the case of frequent weak earthquakes, and for a significant number of stronger and possible very strong and destructive earthquakes.

The HS-MG energy dissipation prototype device was created through special design process providing consistent characteristics of all constituent parts. The specific properties of the created HS-MG unit, that was constructed and used in testing shaking table bridge model, are as follows:

a) Base plate with a side support system

The lower structure segment comprises a rigid metal base ring, (1) in Figure 1, with the diameter of 780 mm, width of 155 mm, and thickness of 25 mm, in which are fixed eight solid hexagonal metal side vertical supports, (2) in Figure 1, having heights of 220 mm and cross-sections formed based on dimensions of 65.0 mm, representing the distance between two parallel section sides. At the upper end, these octagonal vertical supports are connected to a metal ring plate (6), also having the diameter of 780 mm, thickness of 10.0 mm, and width of 85 mm. The metal side vertical supports were provided with openings at two levels, namely, the first eight at level-1 and the second eight at level-2, through which the special supporting devices are fixed, (5) in Figure 1. Accordingly, three supporting modes of the HS energy dissipation (ED) components could be provided, including: c) support without a gap; d) support with GAP-G1, and e) support with GAP-G2, Figure 2.

b) Central activating system

The upper structure segment of the HS-MG device is formed of a central circular metal element with the diameter of 90 mm and height 200 mm. On the upper side, the central stiff element is fixed to the square metal end-plate with openings, having dimensions of 400 mm x 400 mm and thickness of 20 mm. This plate serves for fixation of the central element (representing a rigid cantilever) to the upper isolated super-structure. Formed at the corresponding heights of level-1 and level-2 are the respective supports around the central element formed by welding of two hollow metal rings having side diameter of 182 mm and thickness of 12 mm. Both were provided with eight openings forming hinged support. At each level, there are regularly distributed eight supports with supporting modes without a gap (hinge supports) for the connected horizontal HS-MG energy dissipation components. The described first segment of the HS-MG device is fixed to the lower segment of the bridge structure through its base plate. The second structural segment of the HS-MG device is fixed to the upper seismically isolated RC slab of the bridge model through its end metal plate;

c) Horizontal HS energy dissipation components

Installed between the two basic segments (a) and (b), at both device levels, are a series of eight HS-MG energy dissipation components, presented in Figure 1 (left and right), Figure 2, and Table 1. Their supports toward the central part were mechanically made in the form of an ideal hinge without a gap. However, the channel-shaped external supports were specifically designed and constructed, Figs. 2 (d and e), to provide the specified starting gap of G1 = 5.5 mm at level-L1 and of G2 = 18.5 mm at level-L2, respectively at both sides from considered initial position of movable steel pins. The full, two-side gap appears to be double in both considered cases. By integration of the three segments, an original compact HS-MG energy dissipation device was assembled.

The created structure of such a specific energy dissipation system actually exhibited an assured specific capability to be adaptively activated depending on the earthquake intensity level, following the successive activation of the HS-MG components installed with different gap sizes.

In total, six different prototype models of horizontal S-shaped (HS-MG) energy dissipation components were designed and constructed. These were classified into two groups according

Table 1. Prototype models of HS-MG components

No.	Label	L [mm]	d_0 [mm]	d_1 [mm]	d_2 [mm]	n
1	HS-1.1	180	18.0	25.0	30.0	25
2	HS-1.2	180	12.0	18.6	23.0	25
3	HS-1.3	180	12.0	15.0	23.0	25
4	HS-2.1	150	18.0	25.0	30.0	25
5	HS-2.2	150	12.0	18.6	23.0	25
6	HS-2.3	150	12.0	16.0	23.0	25

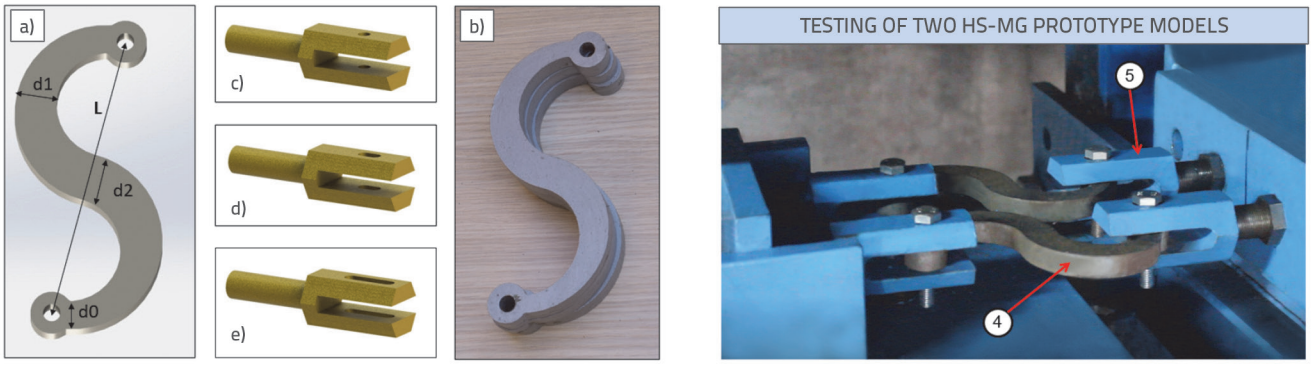

Figure 2. Parameters of constructed and tested HS-MG prototype components: HS-MG components and supporting devices (left); Test setup for testing of two HS-MG prototype models (right)

to the span of the centres of their supporting openings of 180 and 150 mm. The prototype models of the HS-MG energy dissipation components were designed to have double-semi-circular forms and to be produced using ductile sheet metal with the thickness of 15.0 mm. Variable height of the cross-section was adopted considering a smaller dimension d_0 in the vicinity of the openings and including properly increased dimensions to d_1 and d_2 along the semi-circular arches (Figure 2). The number of produced specimens of each prototype model was quite large (n = 25) to realize the planned series of tests on components and devices considering different gaps and test conditions. For shaping of the complex forms of the HS-MG components, precise technology was adopted to eliminate surface roughness and avoid possible failure during their multi-cyclic compressive and tensile deformation. In fact, during the manufacturing process, a CNC-machine was employed for computer-based shaping of the form, while precise cutting was conducted using the "water-jet" technology with a very small speed providing high precision and continuity of the cross-sectional areas.

3.2. Testing of HS-MG devices

Before implementation of the HS-MG devices in the bridge model used for shaking table testing, their constructed prototypes were tested under quasi-static cyclic loads. The quasi-static tests included cyclic testing of:

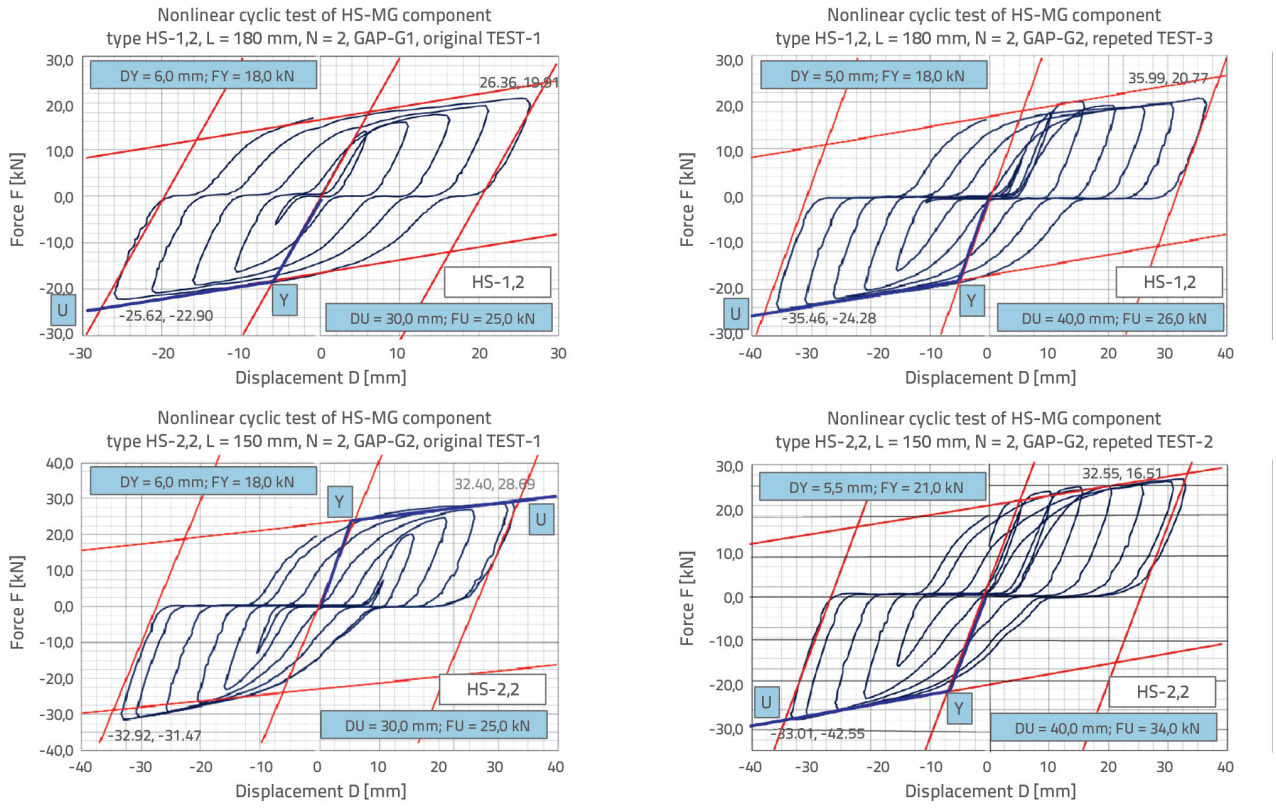

Figure 3. Hysteretic response of tested characteristic types of HS-MG components: (1) Component HS-1.2 tested with gap-G1 and gap-G2 (up); (2) Component HS-2.2 tested with gap-G2 (down)

- seismic isolation DSRIB devices
- selected components of devices for energy dissipation.

Displacement cyclic loading with increasing amplitudes was used for all quasi-static tests, Figure 2 (right). Each HS-MG component was tested twice or three times. The first TEST-1 was referred to as the original test, while TEST-2 and TEST-3 represented repeated tests.
For testing of six HS-MG components under cyclic loads, simulating GAP-G1 and GAP-G2, twelve components were used. With the anticipated realization of the original and the repeated tests of each component, a total of 24 nonlinear cyclic tests were completed. Following processing and plotting of the extensive data volume recorded from the tests, high energy dissipation capacity was observed in all cases. Figure 3 shows the experimentally defined typical hysteretic responses of the tested two HS-MG components. The main parameters controlling the hysteretic responses in both cases are very similar. In the case of tested component type HS-1.2, in both cases there was no difference in the yield force, while the yield displacements varied insignificantly. The lower part of Figure 3 comparatively presents the original hysteretic responses obtained from the conducted two nonlinear cyclic tests of the same component type HS-2.2, firstly tested with simulated GAP-G2 and then again tested with the same simulated GAP-G2 (repeated test). The obtained main parameters controlling the hysteretic responses in both cases were also very similar. The difference in yield force was less than 9 %, while the recorded yield displacements were similar. From the conducted original experimental study, important observations and conclusions can be drawn:

- The observed hysteretic response of the HS-MG components appeared quite stable, indicating almost unchanged controlling parameters in the course of full sequences of repeated cycles
- The resulting shape of the hysteresis was distinctively modified according to the size of the simulated gap-based cyclic response
- It was confirmed that nonlinear cyclic response could be very well analytically represented by the bi-linear model
- The compact HS-MG device exhibited an advanced, adaptable nonlinear behaviour, with high energy dissipation capability.

4. Refined modelling of HS-MG prototype components

Analytical simulation of specific, gap-based hysteretic response of HS-MG prototype components represented an important study step. Following the stated important goals, a programmed, specifically targeted research based on the implemented refined (micro) modelling, applicable for realistic simulation of the nonlinear response of the innovative prototypes of HS-MG components, was conducted, Figure 4.
Steel of S355 class was modelled by solid elements considering a bilinear kinematic hardening material model. For the linear-elastic domain, considered was a modulus of elasticity E1 = 200G Pa and Poisson's coefficient ν = 0.3.

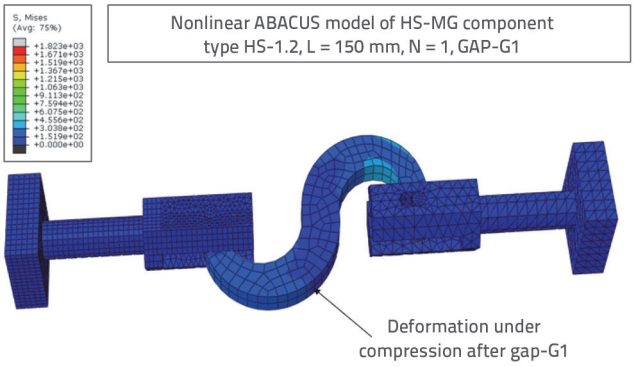

Figure 4. Formulated refined 3D Abacus model of HS-MG energy dissipation component type HS-2.2 with GAP-G1

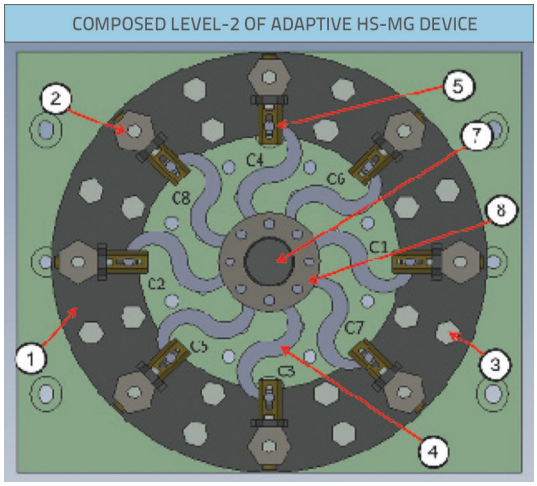

Figure 5. Typical installation of ED components with GAP-G1 at level-2

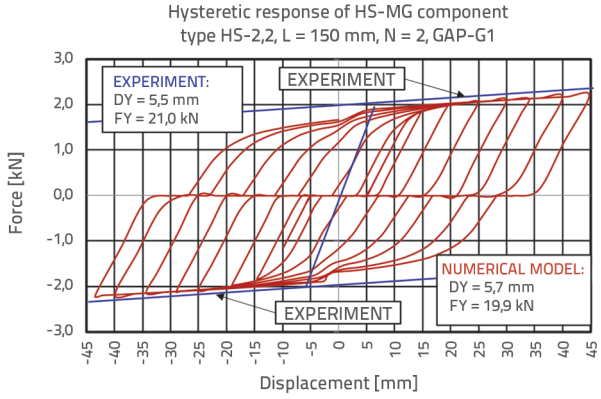

Figure 6. Computed theoretical hysteretic response of HS-2.2 component under simulated cyclic loads and GAP-G1, compared with the experimentally defined envelope lines

conditions for effective controlling of the energy dissipation capacity were provided in any arbitrary direction. Such original, highly important characteristics are effectively mobilized in a compact device with the used set of radially-spaced HS-MG components, representing the essential energy dissipation part of any assembled multi-gap and multi-directional devices with a pre-defined gaps in two

levels, Figure 5. The refined 3D mathematical model, Figure 4, was formulated in Abacus for the HS-MG component of the type of HS-2.2 with GAP-G1. By setting the actual material characteristics, as well as providing a refined discretization model, provided were conditions for solution with high accuracy. Generally, if it is compared with original experimental results, quite small differences were observed, being in the range of 2 to 7 %. With the applied nonlinear micro-model, the specific prototype components were analysed considering different gaps G1 & G2. The example of the resulting specific gap-based hysteretic response computed numerically for the HS-MG energy dissipation component type HS-2.2 under simulated cyclic loads, according to the pre-defined displacement protocol and side-support with GAP-G1, is presented in Figure 6, together with the comparative bi-linear envelope lines obtained from the conducted experimental reversed-cyclic test. The defined differences between the experimental and numerical results are evidently insignificant.

5. Isolation and displacement limiting devices

5.1. Testing of DSRIB isolation devices

The present isolation system used for the experimental GHS bridge model was assembled by use of the developed models of double spherical rolling isolation bearing (DSRIB) devices having two large-radius of spherical surfaces (Figure 7).

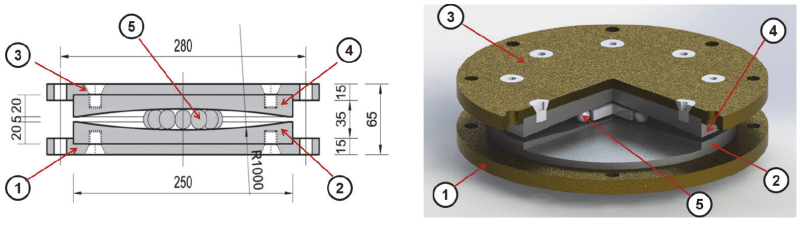

Figure 7. Elements of constructed and used prototypes of DSRIB devices

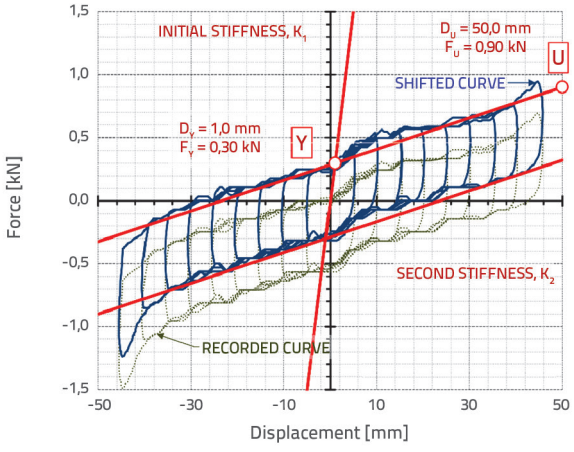

Figure 8. Typical response of DSRIB device

By the advanced gapped form of hysteretic response of each HS-MG component, The DSRIB devices were originally designed, constructed and used in previous investigation Ristic, J., et al., 2017, [35].

The targets set before for design and construction of the device were fulfilled: (1) very small horizontal reaction and friction forces (reaching maximum 4.2 % of the vertical load), and (2) stable hysteretic behaviour along the entire range of large displacements were achieved, Figure 8.

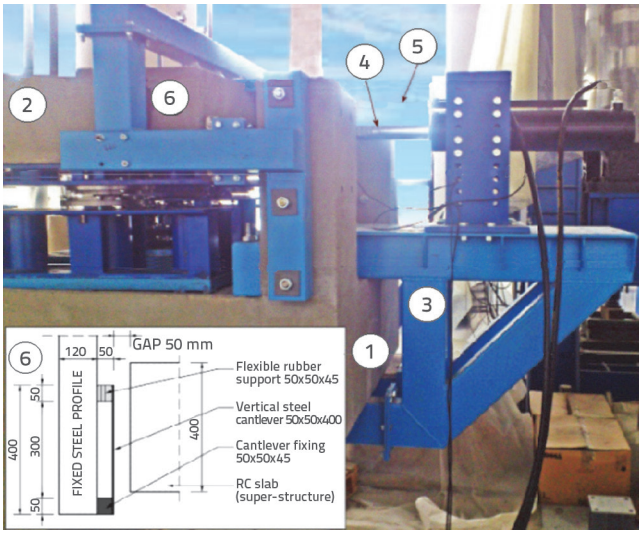

Figure 9. DLD and actuator position

5.2. Displacement limitation devices

The implemented DL system, in the model, consisted of built-in four limiting devices in the form of short flexible steel cantilevers supported by a rubber block (Figure 9, part 6), acting as stoppers, Ristic, J., et al., 2021, [36]. In practice, new specially designed rubber buffers can be advanced solution.

6. Seismic tests of large-scale GHS bridge model

6.1. Construction of GHS bridge prototype model

The design and construction of the test model of the innovative GHS bridge prototype represented a complex and specific process, specifically focused on assuring conditions for realistic experimental simulation of pre-defined important testing requirements. The three basic data-sets, including (a) The main characteristics of the GHS bridge model; (b) Available size of the seismic shaking table and (c) Implemented instrumentation system of the GHS bridge model, are accordingly presented in [36, 37]. For this study purposes, the originally constructed large RC substructure and superstructure segments were used as identical. The new GHS bridge test model used in this study was assembled with installation of the

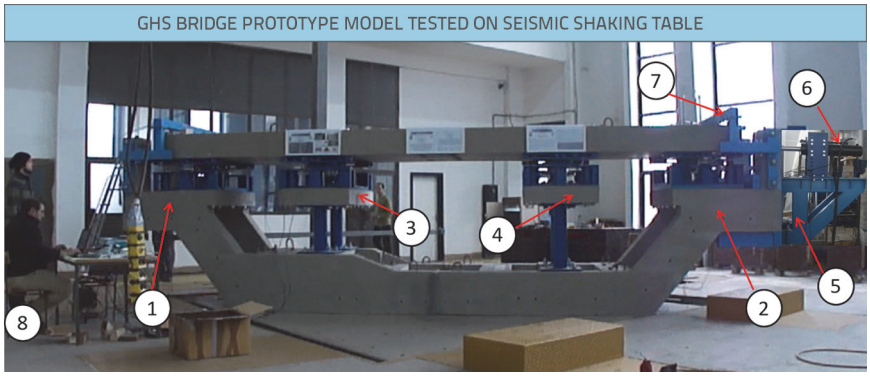

Figure 10. GHS bridge prototype model: (1) left end support; (2) right end support; (3) support above the shorter piers; (4) support above the longer piers; (5) actuator supporting structure; (6) actuator; (7) support of DL devices; (8) computer controlling the cyclic tests

newly created innovative HS-MG device for energy dissipation. A brief description of the basic GHS model geometry, principal model characteristics and the adopted instrumentation system is included to assist in successful following the obtained results from the present new tests.

Following the specific study objectives, a common three-span bridge prototype having two rigid end abutments and two flexible middle piers was selected as appropriate. The total length of the selected bridge prototype was L = 15.75+27.00+15.75 = 58.50 m. The two pairs of middle piers were considered to be of different heights, h1 = 9.50 m and h2 = 11.70 m, simulating their different stiffness. The bridge superstructure consisted of a rigid RC deck, which was intentionally spaced at an appropriate distance from the substructure bents in order to accommodate the constituent devices of the test model. The bridge deck rested on the two abutments via movable bearings and on the middle piers, through hinge type supports. For the purposes of the shaking table test, the experimental GHS bridge test model was designed as geometrically reduced in relation to the selected prototype bridge. Regarding the shaking table dimensions, its loading capacity and related characteristics, a geometric scale factor, l_r = 1:9 was adopted. In order to preserve the model similarity, all the other characteristics related to the dynamic tests needed to be properly scaled. Considering the important factors addressed, the combined true replica-artificial mass simulation model was adopted as the most adequate. The scale factors for different physical quantities are defined as a function of geometrical scale factor, according to the similitude law [38]. Following the characteristics of the selected bridge prototype and respecting the design parameters, the experimental GHS bridge model was designed to provide, as much as possible, realistic conditions [35, 39, 40]. The bridge model, Figure 10 and Figure 11, actually represent a structure having rigid abutments and flexible middle piers. Also, the model could be used as a single-span structure, when middle piers were not considered. The abutments and the substructure segment were designed as robust RC elements. The steel-tube middle piers represented columns with different stiffness. Presently, tested was one-span bridge model option, because the effect of middle piers was not included. The superstructure of the model was constructed as a rigid slab whose total height was conveniently enlarged to enable simulation of the total mass and large generated inertial forces. The total length of the model sub-structure amounted to 8.30m. The total width of the model was 1.50 m.

At both ends spaced were RC slabs, providing sufficient space for the installation of pairs of DSRIB isolators and the new HS-MG devices for energy dissipation between them, as indicated in Figure 12.

The displacement limiting (DL) devices were designed in the form of 400 mm long vertical steel cantilevers fixed at the lower end and supported by a 50/50 mm rubber block at the upper end (schematically shown in Figure 9, part 6). The DL devices were installed at 50mm gaps from the RC superstructure to prevent destructive effects from potential excessive displacements.

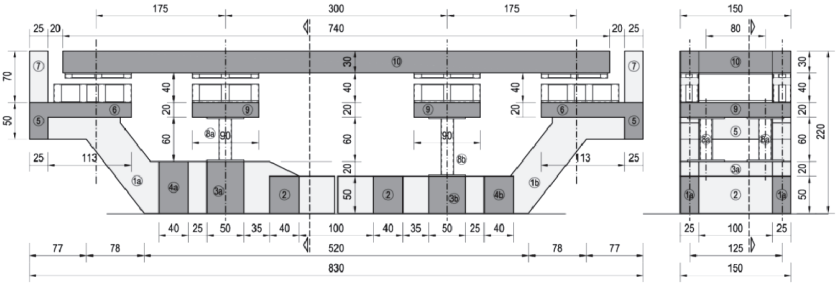

Figure 11. Longitudinal and transversal sections of the GHS bridge model

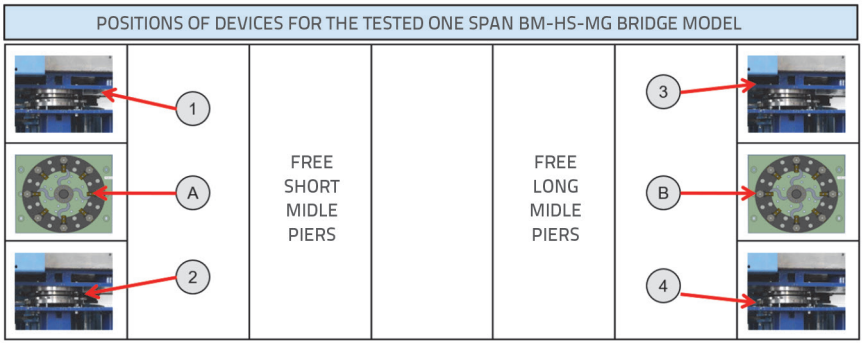

Figure 12. Positions of DSRIB devices (1 to 4) and the new HS-MG devices (A and B)

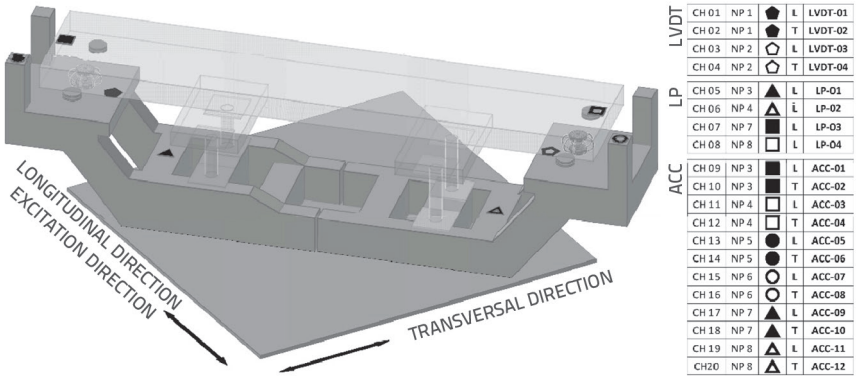

Figure 13. Acquisition points with sensors and recording channels

All steel parts were manufactured to a reduced scale by use of S355 steel material, while concrete C25/30 was used for construction of all RC parts of the constructed bridge model.

The existing laboratory seismic shaking-table was square-shaped (5.0 by 5.0 m). Seismic input could be applied in one horizontal and in vertical direction. To adapt the large-scale GHS bridge model for seismic testing, its longitudinal axis was positioned along the diagonal of the shaking table (Figure 10). In that way, generation of seismic forces was enabled in longitudinal and transverse direction of the bridge model. The bridge test model was assembled on the shaking table and equipped with the defined instrumentation. For seismic testing of the GHS system, the model deck rested on four DSRIB isolators spaced at the two abutments (using two pairs of devices, Figure 12 (1 to 4). Having excluded middle piers, tested was the resulting single-span bridge model. The two HS-MG devices (A and B) were installed at the respective abutment positions, Figure 12. To ensure acquisition of all the required data during the dynamic tests, a well-designed instrumentation system was installed. It consisted of the following three different types of sensors, Figure 13. The integral instrumentation system was before used and presented in details [35]. For this experimental study purposes, identical instrumentation system was adopted and successfully used.

Four transducers of the type of LVDT were used for recording time histories of relative displacements between the sub- and super- structure. Four transducers of the type of LP (linear potentiometer) were used for measurement of absolute displacements of the model by fixing one of its ends to fixed points (beyond the shaking table). Twelve sensors of the type ACC (acceleration sensors) were used to record the time histories of acceleration in longitudinal and transverse direction of the selected six characteristic points of the model.

6.2. Seismic shaking table tests of GHS bridge model

a) Model assembling

The innovative GHS bridge prototype model shown in Figure 12 was specifically assembled, incorporating four DSRIB isolation devices, two new HS-MG energy dissipation devices and four displacement limiting devices (DLDs), Figure 9. The created HS-MG energy dissipation devices were composed with installation of pre-selected suitable prototypes of energy dissipation components of the type of HS-1.2, Table. 1. The selected HS-MG components were installed at two levels considering two different pre-defined gaps of the size of G1 = 5.0 mm and G2 = 18.0 mm, respectively. Regarding the model similarity rules, the final set of HS-MG devices was created by respective installation of four, radially distributed components of the type of HS-1.2, at each level, Figure 12.

b) Sine-sweep tests

With the conducted dynamic tests with simulated sine-sweep dynamic inputs, 0.02g and 0.05g, covering a range of frequencies (1–35 Hz) and using the provided data sources, defined were: (1) the initial fundamental period amounting to T_o = 0.522 s, corresponding to the case of the bridge model with installed DSRIB devices only. The installed HS-MG devices were not activated due to the present gaps; and (2) Damping amounting between 3.0 and 3.5 %.

c) Comparative testing

To assess the contribution of the HS-MG devices for energy dissipation, the bridge was first tested with installed DSRIB isolators only, under simulated El Centro earthquake scaled to PGA = 0.81 g. The comparative relative displacements recorded under equal test conditions for the system composed with and without HS-MG devices are presented in Figure 15. It may be noticed that bridge model having installed HS-MG devices actually represented a highly favourable upgrading option. For example, unacceptable relative displacement of De = 42.34 mm was obtained for the system with seismic isolation only. However, considering the GSH system with new HS-MG devices, the relative displacement was reduced to a fully controlled value of Dc = 21.97 mm, representing an important reduction of 48.1 %. The excessive response recorded for bridge model with isolation only, actually showed its critical state, since the displacement limit of the seismic isolators was 40.0 mm.

d) Brief presentation of testing conditions and selected results, including

d-1) Seismic input

Seismic testing of the new GHS bridge model was performed regarding four real earthquake records. However, to obtain representative experimental data, strong earthquake intensities were considered in all testing cases. High seismic input intensities were generated considering high values of peak ground accelerations amounting to PGA = 0.81g for the El Centro (1940) record, PGA = 0.77g for the Petrovac (Montenegro, 1979) record, PGA = 0.70g for the Landers record and PGA = 0.98g

Table 2. Maximum relative displacements recorded from the four original GHS bridge model tests

No.	O-T1: C-El-Centro, PGA = 0.81g			O-T2: C-Petrovac, PGA = 0.77g		
	Channel	Dmax (-) [mm]	Dmax (+) [mm]	Channel	Dmax (-) [mm]	Dmax (+) [mm]
1	LVDT-03	-21.97	18.91	LVDT-03	-12.50	19.59
2	LVDT-04	-6.33	4.15	LVDT-04	-5.88	7.60
No.	**O-T3: C-Landers, PGA = 0.70g**			**O-T4: C-Northrige, PGA = 0.98g**		
	Channel	**Dmax (-) [mm]**	**Dmax (+) [mm]**	**Channel**	**Dmax (-) [mm]**	**Dmax (+) [mm]**
1	LVDT-03	-21.46	21.76	LVDT-03	-19.40	25.58
2	LVDT-04	-2.07	17.95	LVDT-04	-6.40	7.16

for the Northridge record, respectively. Following the similitude law. the original earthquake records were time compressed for a time factor of 1/3, as a square root of lr.

d-2) Data acquisition

Due to the complexity of the tests, extensive experimental data files were recorded from each acquisition channel. The integral data recording system included the full set of 20 channels instrumented with sensors according to the model instrumentation plan and additional extra sensors are used for full controlling of the shaking table. Having such an extensive instrumentation system and refined data sampling rate from each seismic test, approximately 5 million numerical values were recorded. The testing process, containing nine seismic tests, was completed very successfully, and all sensors provided continuously correct and complete experimental records. The representative results showing the actual system response were selected, and are presented and discussed herein.

d-3) Relative displacements

The relative peak displacements, including positive and negative pulses, recorded from the seismic tests of the GHS system under the simulated El-Centro, Petrovac, Landers, and Northridge earthquakes are presented in Table 2. Comparatively, Figure 14 (left) shows the time-histories of the recorded superstructure relative displacement responses in the longitudinal (L) and transverse (T) directions during the tests conducted by simulation of the strong El-Centro, Petrovac, and Northridge earthquakes, respectively. Regarding the experimental results, the following important observations were made: (1) The recorded displacements in the L direction (direction of earthquake excitation) are dominant; (2) The recorded displacements in the T direction normal to the earthquake excitation are small and insignificant; (3) The absolute maximum of recorded relative displacement amounting to Dmax = 25.58 mm was below the critical (allowable) relative displacement of the seismic isolators amounting to Da = 40.0 mm, and (4) Generally, the seismic response of the assembled GHS system that was tested twice appeared to be very similar. The original results from the conducted original series of tests-1 are presented in Table 2). Consequently, the series of repeated seismic tests-2 (not presented) were realized using the same four earthquakes. Only small, negligible differences in the maximum displacements were observed.

d-4) Accelerations

The representative peak accelerations recorded by sensors ACC-01, ACC-03, and ACC-05 in the L-direction, during the GHS model seismic tests conducted under the simulated El-Centro and Petrovac earthquakes, are shown in Table 3. Sensors ACC-01 and ACC-03 were located on the left and right superstructure end, while ACC-05 was spaced on the sub-structure segment (Figure 13). Comparatively, Figure 14 (right) shows the time-histories of the recorded acceleration responses by ACC-03 in the longitudinal direction and ACC-04 in the transversal direction during the tests conducted by simulating the strong El-Centro, Petrovac, and Northridge earthquakes, respectively. Considering the presented results, it was confirmed again that:

- The presented acceleration histories recorded at the superstructure in the L-direction were dominant
- The recorded accelerations at the substructure and in the T-direction were smaller and in the expected range;
- The new GHS system exhibited the respective property of sustainability as the response parameters recorded during the original tests-1 and the repeated tests-2 were quite similar
- The presented values of dynamic amplification factor (DAF) also given in Table 3 demonstrate a favourable and consistent response. The obtained relations between the maximum response and maximum input acceleration (DAF = MaxA/PGA) are within the expected ranges in all cases.

d-5) Absolute displacements

The recorded absolute displacement responses (in the L-direction) by the LP sensors, installed on the sub- and super-structure segments, prove that full control of the shaking table was successful in all realized testing cases.

d-6) System advances

Generally, the new GHS bridge system showed safe and very favourable behaviour under strong earthquake excitations.

Table 3. Recorded maximum accelerations during the original GHS model tests conducted under the simulated strong El-Centro and Petrovac earthquakes

No.	O-T1: C-El-Centro, PGA = 0.81g					O-T2: C-Petrovac, PGA = 0.77g				
	Channel	MaxA g (-)	DAF	MaxA g (+)	DAF	Channel	MaxA g (-)	DAF	MaxA g (+)	DAF
1	ACC-01	-1.03	1.27	0.88	1.08	ACC-01	-0.71	0.92	0.73	0.94
2	ACC-03	-1.43	1.76	1.20	1.48	ACC-03	-1.61	2.09	1.24	1.61
3	ACC-05	-0.86	1.06	0.77	0.95	ACC-05	-0.54	0.70	0.53	0.68

Considering the processing of more than 75.000.000 recorded original numerical values obtained from the realized fifteen shaking table tests, the main qualitative advances of the innovative GHS bridge system upgraded with HS-MG energy dissipation devices are summarized in Figure 15.

Stable, reliable, and safe seismic response was observed in all test cases due to the provided significant reduction of maximum relative displacements amounting to 45.1 %, 51.0 %, 45.6 %, and 36.0 %, respectively, in the case of the simulated El Centro, Petrovac, Landers, and Northridge earthquakes. All recorded peak values are lower than the design-defined allowable displacement Da = 40.0 mm for the seismic isolators. The importance of upgrading isolated bridges using the new HS-MG devices was experimentally validated and confirmed with the conducted initial quantification test of the model with the installed seismic isolation only. Under the simulated strong El-Centro earthquake, the tested system

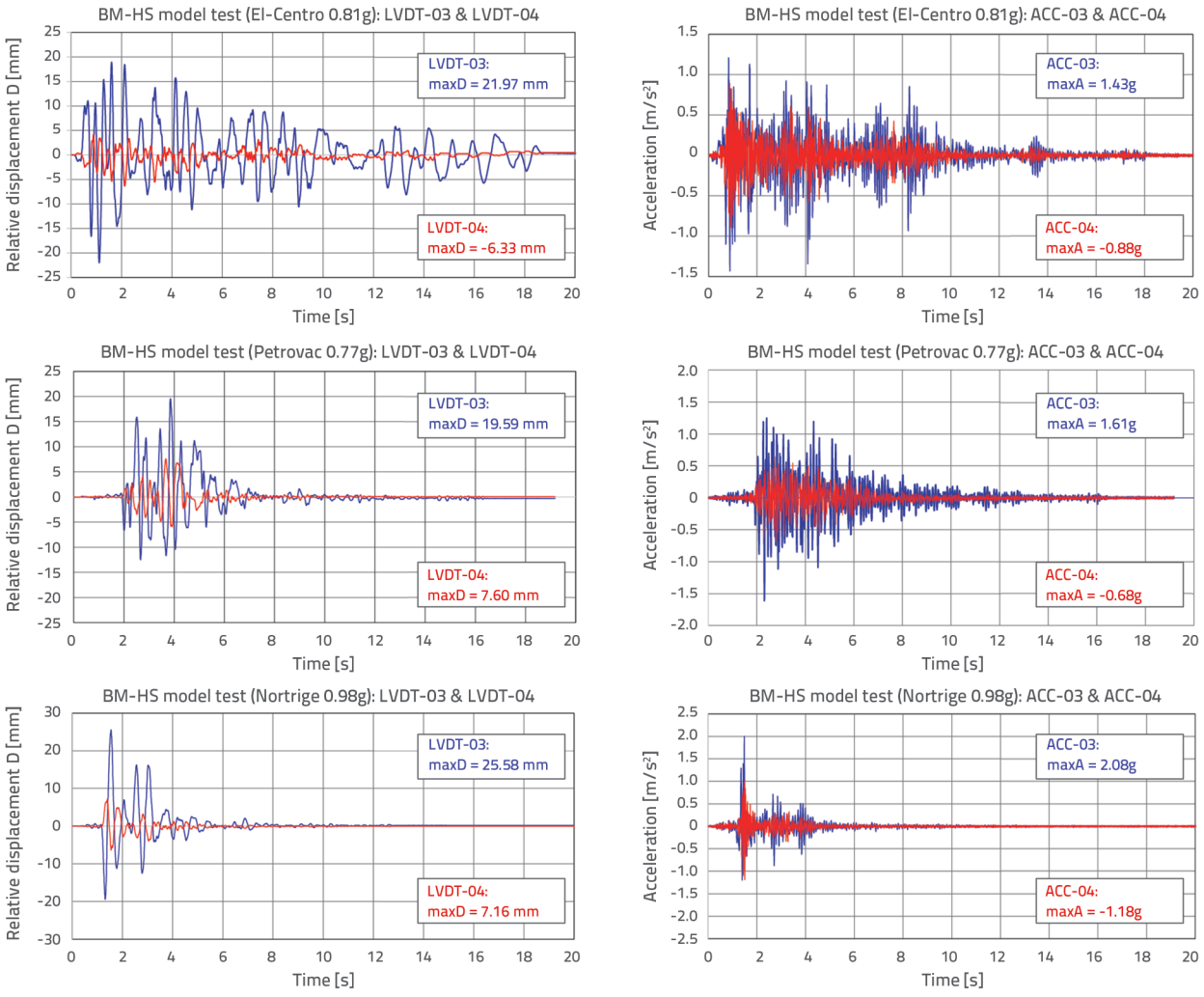

Figure 14. Maximum superstructure relative displacements (left) and acceleration responses recorded by ACC-03 & ACC-04 (right) during the GHS model tests conducted under the simulated strong El-Centro, Petrovac and Northridge earthquakes

without HS-MG devices showed an unsafe response due to the recorded excessive relative displacement amounting to Dmax = 42.34 mm (Figure 15 (left)).

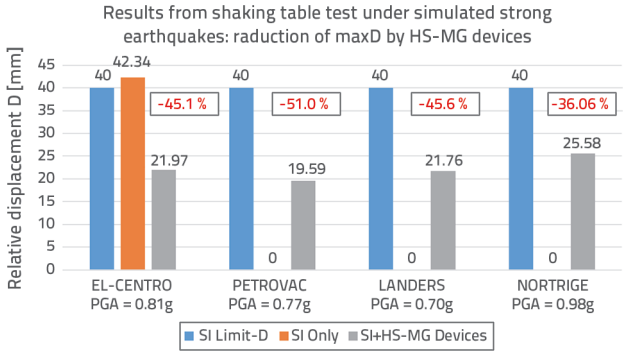

Figure 15. Advances of the GHS bridge system upgraded with HS-MG devices: Reduction in maximum relative displacements defined from the bridge model seismic tests under the simulated real strong earthquakes

7. Conclusions

Considering the results obtained from the conducted extensive, innovative experimental and analytical studies, the following conclusions were derived:

(1) The new GHS system represents a favourable and experimentally proved upgraded option for commonly isolated bridges. The system shows significant modification of the seismic response needed for efficient protection of bridges subjected to repeated and very strong earthquakes; (2) The implemented DSRIB isolation devices were confirmed as favourable isolation bearings for new GHS bridges. However, the other types of isolation bearings may also be regarded as a potentially good application option; (3) The created uniform multi-gap HS-MG energy dissipation devices presented very good energy dissipation capacity and exhibited stable hysteretic response under arbitrary earthquake excitation. In addition, the new HS-MG devices preserve their dissipation characteristics even in the cases of intensive repeated cyclic earthquake loading; (4) The displacement limiting (DL) devices should be an obligatory constituent system of GHS bridges against excessive displacements of the bridge superstructure. Their appropriate design ensures their activation only in the critical cases of very strong specific earthquakes. Further, their activation will provide important improvement of the bridge seismic safety under critical earthquake events; (5) Hysteretic, gap-based response of HS-MG components and devices can be successfully predicted by application of the micro-modelling concept and with application of bilinear kinematic hardening material model; (6) The present research resulted in experimentally proved background research sources providing conditions for elaboration of respective design rules assuring implementation of the new GHS system with advanced, qualitatively upgraded seismic protection of bridge structures in seismic regions.

Acknowledgements

The present study represents part of the NATO Science for Peace and Security Project: Seismic Upgrading of Bridges in South-East Europe by Innovative Technologies (SFP: 983828). The extended NATO support to the realization of the present innovative research is highly appreciated.

REFERENCES

[1] Kelly, J.M.: Aseismic Base Isolation: A Review and Bibliography, Soil Dynamics and Earthquake Engineering, 5 (1986), pp. 202-216

[2] Kunde, M.C., Jangid, R.S.: Seismic Behavior of Isolated Bridges: A-State-of-the-art Review, Electronic Journal of Structural Engineering, 3 (2003), pp. 140-170

[3] Turkington, D.H., Carr, A.J., Cooke, N., Moss, P.J.: Seismic design of bridges on Lead-rubber bearings, Journal of Structural Engineering, 115 (1989), pp. 3000-3016

[4] Robinson, W.H.: Lead-Rubber Hysteretic Bearings Suitable for Protecting Structures During Earthquakes, Earthquake Engineering and Structural Dynamics, 10 (1982), pp. 593-604

[5] Dolce, M., Cardone, D., Palermo, G.: Seismic Isolation of Bridges Using Isolation Systems Based on Flat Sliding Bearings, Bulletin of Earthquake Engineering, 5 (2007), pp. 491–509

[6] Iemura, H., Taghikhany, T., Jain, S.K.: Optimum Design of Resilient Sliding Isolation System for Seismic Protection of Equipment, Bulletin of Earthquake Engineering, 5 (2007), pp. 85–103

[7] Kartoum, A., Constantinou, M.C., Reinhorn, A.M.: Sliding Isolation System for Bridges: Analytical Study, Earthquake Spectra, 8 (1992), pp. 345-372

[8] Wang, Y.P., Chung, L., Wei, H.L.: Seismic Response Analysis of Bridges Isolated with Friction Pendulum Bearings, Earthquake Engineering and Structural Dynamics, 27 (1998).

[9] Zayas, V.A., Low, S.S., Mahin, S.A.: A Simple Pendulum Technique for Achieving Seismic Isolation, Earthquake Spectra, 6 (1990), pp. 317-334

[10] Mokha, A., Constantinou, M.C., Reinhorn, A.M.: Teflon Bearings in Seismic Base Isolation I: Testing, Journal of Structural Engineering, 116 (1990), pp. 438-454

[11] Constantinou, M.C., Kartoum, A., Reinhorn, A.M., Bradford, P.: Sliding Isolation System for Bridges: Experimental study, Earthquake Spectra, 8 (1992), pp. 321-344

[12] Xiang, N., Yang, H., Li, J.: Performance of an Isolated Simply Supported Bridge Crossing Fault Rupture: Shake Table Test, Earthquakes and Structures, 16 (2019) 6

[13] Skinner, R.I., Kelly, J.M., Heine, A.J.: Hysteretic Dampers for Earthquake Resistant Structures, Earthquake Engineering and Structural Dynamics, 3 (1975), pp. 287-296

[14] Guan, Z., Li, J., Xu, Y.: Performance Test of Energy Dissipation Bearing and Its Application in Seismic Control of a Long-Span Bridge, J. of Bridge Eng., 15 (2010).

[15] Ene, D., Yamada, S., Jiao, Y., Kishiki, S., Konishi, Y: Reliability of U-shaped Steel Dampers Used in Base-Isolated Structures Subjected to Biaxial Excitation, Earthquake Engineering & Structural Dynamics, 46 (2017), pp. 621–639

[16] Oh, S., Song, S., Lee, S., Kim, H.: Experimental Study of Seismic Performance of Base-Isolated Frames with U-shaped Hysteretic Energy-Dissipating Devices, Engineering Structures, 56 (2013), pp. 2014-2027

[17] Jiao, Y., Kishiki, S., Yamada, S., Ene, D., Konishi, Y., Hoashi, Y., Terashima, M.: Low Cyclic Fatigue and Hysteretic Behavior of U-shaped Steel Dampers for Seismically Isolated Buildings under Dynamic Cyclic Loadings, Earthquake Engineering Structural Dynamic, 44 (2014) 10, pp. 1523–1538

[18] Jankowski, R., Seleemah, A., El-Khoribi, S., Elwardany, H.: Experimental Study on Pounding between Structures During Damaging Earthquakes, Key Engineering Materials, 627 (2015), pp. 249-252

[19] Tubaldi, E., Mitoulis, S.A., Ahmadi, H., Muhr, A.: A Parametric Study on the Axial Behavior of Elastomeric Isolators in Multi-Span Bridges Subjected to Horizontal Seismic Excitations, Bulletin of Earthquake Engineering, 14 (2016), pp. 1285–1310

[20] Serino, G., Occhiuzzi, A.: A Semi-Active Oleodynamic Damper for Earthquake Control: Part 1: Design, Manufacturing and Experimental Analysis of the Device, Bulletin of Earthquake Engineering, 1 (2003), pp. 269–301

[21] Kataria, N.P., Jangid, R.S.: Seismic Protection of the Horizontally Curved Bridge with Semi-Active Variable Stiffness Damper and Isolation System, Advances in Structural Engineering, 19 (2016) 7, pp. 1103-1117

[22] Mayes, R.L., Buckle, I.G., Kelly, T.E., Jones, L.R.: AASHTO Seismic Isolation Design Requirements for Highway Bridges, Journal of Structural Engineering, 118 (1992), pp. 284-304

[23] NHI: LRFD Seismic Analysis and Design of Bridges, Reference Manual: NHI Course No. 130093 and 130093A, National Highway Institute, U.S. Department of Transportation, 2014.

[24] Unjoh, S., Ohsumi, M.: Earthquake Response Characteristics of Super-Multispan Continuous Menshin (Seismic Isolation) Bridges and the Seismic Design, ISET J. of Earthquake Engineering Technology, 35 (1998), pp. 95-104

[25] Tian, L., Fu, Z., Pan, H., Ma, R., Liu, Y.: Experimental and Numerical Study on the Collapse Failure of Long-Span Transmission Tower-Line Systems Subjected to Extremely Severe Earthquakes, Earthquakes and Structures, 16 (2019) 5

[26] UNCRD: Comprehensive Study of the Great Hanshin Earthquake, UNCRD Research Report Series No. 12, United Nations Centre for Regional Development (UNCRD), Nagoya, Japan, 1995.

[27] NIST: The January 17, 1995 Hyogoken-Nanbu (Kobe) Earthquake: Performance of Structures, Lifelines, and Fire Protection Systems, NIST SP 901, U.S. Department of Commerce, Technology Administration, Washington, USA, 1996.

[28] Yuan, W., Feng, R., Dang, X.: Typical Earthquake Damage and Seismic Isolation Technology for Bridges Subjected to Near-Fault Ground Motions, 2018 International Conference on Engineering Simulation and Intelligent Control, Hunan, China, 2018.

[29] Aye, M., Kasai, A., Shigeishi, M.: An Investigation of Damage Mechanism Induced by Earthquake in a Plate Girder Bridge Based on Seismic Response Analysis: Case Study of Tawarayama Bridge under the 2016 Kumamoto Earthquake, Adv. in Seismic Performance Assessment and Improvement of Structures, 2018.

[30] Lee, G.C., Kitane, Y., Buckle, I.G.: Literature Review of the Observed Performance of Seismically Isolated Bridges, Multidisciplinary Center for Earthquake Engineering Research, New York, NY, USA, 2001.

[31] Ghasemi, H., Cooper, J.D., Imbsen, R., Piskin, H., Inal, F., Tiras, A.: The November 1999 Duzce earthquake: Post- earthquake Investigation of the Structures on the TEM, Publication No. FHWA-RD-00-146, Federal Highway Administration Report, 2000.

[32] Erdik, M.: Report on 1999 Kocaeli and Duzce (Turkey) Earthquakes, Structural Control for Civil and Infrastructure Engineering, 2001., pp. 149-186

[33] Fujino Y., Siringoringo D.M., Kikuchi M., Kasai K., Kashima T.: Seismic Monitoring of Seismically Isolated Bridges and Buildings in Japan-Case Studies and Lessons Learned; Seismic Structural Health Monitoring, Springer Tracts in Civil Engineering, Springer, Cham., 2019.

[34] Li, X., Shi, Y.: Seismic Design of Bridges against Near-Fault Ground Motions Using Combined Seismic Isolation and Restraining Systems of LRBs and CDRs, Shock and Vibration, (2019), pp.11

[35] Ristic, J., Misini, M., Ristic, D., Guri, Z., Pllana, N.: Seismic Upgrading of Isolated Bridges with SF-ED Devices: Shaking Table Tests of Large-Scale Model, Gradjevinar, 70 (2018) 6, pp. 2147-2017

[36] Ristic, J., Brujic, Z., Ristic, D., Folic, R., Boskovic, M.:Upgrading of isolated bridges with space-bar energy-dissipation devices: Shaking table test, Advances in Structural Engineering, (2021) 6; pp. 2948–2965

[37] Ristic, J.: Modern Technology for Seismic Protection of Bridge Structures Applying Advanced System for Modification of Earthquake Response, PhD Thesis, Institute of Earthquake Engineering and Engineering Seismology (IZIIS), SS Cyril and Methodius University, Skopje, Macedonia, 2016.

[38] Candeias, P., Costa, A.C., Coelho, E.: Shaking Table Tests of 1:3 Reduced Scale Models of Four-Story Unreinforced Masonry Buildings, Proceedings of the 13th World Conference on Earthquake Engineering, Vancouver, 2004., Paper No: 2199

[39] Ristic, D.: Nonlinear Behavior and Stress-Strain Based Modeling of Reinforced Concrete Structures Under Earthquake Induced Bending and Varying Axial Loads, Doctoral Dissertation, School of Civil Engineering, Kyoto University, Japan, 1988.

[40] Ristic, D., Ristic, J.: Advanced Integrated 2G3 Response Modification Method for Seismic Upgrading of Advanced and Existing Bridges, Proceedings of the 15th World Conf. on Earthquake Engineering (WCEE), Lisbon, 2012.